Superior Reinforcement in Melt-Spun Polyethylene/Multiwalled Carbon Nanotube Fiber through Formation of a Shish-Kebab Structure

Fang Mai, Ke Wang, Meijun Yao, Hua Deng,* Feng Chen, and Qiang Fu*

College of Polymer Science and Engineering, State Key Laboratory of Polymer Materials Engineering, Sichuan University, Chengdu 610065, People's Republic of China

Received: March 5, 2010; Revised Manuscript Received: May 5, 2010

The formation of a shish kebab (SK) structure, where carbon nanotubes (CNTs) serve as shish and polymer lamellae serve as kebab, is particularly interesting and provides a novel way to enhance the polymer−CNT interface. A fine SK structure is achieved through melt spinning. High density polyethylene and pristine CNTs were first compounded in an extruder. The compound was then spun into fibers with different draw ratios with the aid of a capillary rheometer. The crystalline structure and mechanical behavior were characterized by scanning electron microscopy, differential scanning calorimetry, two-dimensional wide-angle X-ray scattering, polarized Raman spectroscopy, and tensile testing. An increase in tensile strength as high as 3 times has been achieved in the fiber. The formation of SKs is considered as the main mechanism responsible for the enhanced interfacial interaction and excellent tensile property.

1. Introduction

Carbon nanotubes (CNTs) are widely used to improve different properties in various polymers, including mechanical properties,[1−3] thermal stability,[4] and electric conductivity.[5,6] However, the problems such as aggregations of CNTs and unfavorable compatibility between nanotubes and polymer matrix (especially polyolefin) still remain as great challenges. In order to overcome these challenges, covalent (chemical) functionalization or noncovalent (physical) modification is often necessary for CNTs before blending them with polyolefin. Park et al.[7] prepared polyethylene (PE)/multiwalled carbon nanotube (MWCNT) composites with uniformly dispersed and PE-coated MWCNTs. It is realized by in situ polymerization of ethylene with Cp_2ZrCl_2 immobilized onto the sidewalls of pristine MWCNTs as a catalyst. The prepared composites showed a dramatic 359% increase in Young's modulus compared with neat polymer. In the study carried out by Yang et al.,[8] PE-grafted MWCNTs (PE-g-MWCNTs) have been prepared by reactive blending PE-g-maleic anhydride with amine-functionalized MWCNTs. It was found that tensile strength, yield stress, Young's modulus, strain at break, and toughness of PE were all improved by adding PE-g-MWCNTs into the system. Furthermore, Blake et al.[9] functionalized MWCNTs using *n*-butyllithium, and then modified MWCNTs were further reacted with chlorinated polypropylene (CPP). The Young's modulus, tensile strength, and toughness increased by several times with additional 0.6 vol % CPP-MWCNTs. Other effective methodologies were also used to improve the dispersion of CNTs. For example, CNTs were dispersed in polypropylene (PP) by latex technology in the work reported by Lu et al.,[10] where excellent dispersion of CNTs has been obtained; Chen et al.[11] obtained good dispersion of CNT by preparing ultrahigh molecular weight PE (UHMWPE)/MWCNT composites through gelation/crystallization from solution, while, in the study by Zhang et al.,[12] a good CNT dispersion was achieved by spraying an aqueous solution of SWCNTs directly onto fine PE powder.

The effect of using functionalization on dispersion and interfacial compatibility has been demonstrated in the literature, but some drawbacks are associated with these strategies. These procedures are often complicated, and the production efficiency is quite low. In contrast, the melt compounding approach is more suitable for abundant manufacture of polyolefin/CNT composites. Nevertheless, the mechanical reinforcing efficiency is relatively weak for melt compounded systems. For example, the increase in Young's modulus was 22% while only 2% in tensile strength for high-density PE (HDPE)/CNT composites;[13] for the injection-molded bars of PP/MWCNT composites, the increase in yield stress was only 20% for composites containing 5 wt % CNT, while the value for Young's modulus is 40%;[14] PE/MWCNT composites were prepared through melt blending in the study reported by McNally et al.;[15] they observed uniform dispersion in the relative low molecular weight matrix. The ultimate tensile strength and elongation at break of the composites decreased with the addition of MWCNTs. The poor mechanical reinforcement of CNTs in the above systems indicates that the interfacial adhesion between CNTs and polymer is insufficient. Therefore, new strategies are required.

It is well-known that CNTs could significantly influence the crystallization behavior of semicrystalline polymers due to their capability to nucleate crystallization.[16−19] Therefore, it is particularly interesting if crystalline polymer chains can be deposited onto the CNT surface through epitaxial crystallization. The formation of so-called SK structure, where CNT formed the "shish" and a polymer single crystal lamella formed the "kebab", provides a novel way to bond polymer with CNTs. The formation of SK structure was first observed in solution crystallization of PE with the presence of CNTs, and likely follows the "size-dependent soft epitaxy" mechanism as suggested by Li et al.[20,21] In general, SK is often observed in a controlled solution crystallization procedure. The crystallization environment can be isothermal[21] or nonisothermal[22] or assisted by supercritical CO_2.[23] Interestingly, it has been summarized that the polymers including PE, nylon 6,6, polyvinyl alcohol

* Corresponding authors. Phone: +86-28-85461795 (Q.F.); +86-28-85460953 (H.D.). Fax: +86-28-85461795 (Q.F.); +86-28-85461795 (H.D.). E-mail: qiangfu@scu.edu.cn (Q.F.); huadeng@scu.edu.cn (H.D.).

10.1021/jp1019944
Published on Web 08/02/2010

(PVA), and polybutylece terephthalate (PBT), which have been used to prepare SK, are all in zigzagged conformation.[22,24] Obviously, the formation of SK can be regarded as a noncovalent modification approach to functionalize CNTs, and particularly, the interfacial adhesion between polymer and CNTs will be substantially enhanced; thus, the mechanical properties would be improved efficiently. Direct formation of SK during melt compounding is more favorable for achieving mechanical reinforcement induced by SK than the approach that added preformed SK into a polymer melt,[25] because the SK structure may possibly be destroyed by melting the polymer kebabs on CNTs in the latter case. Recently, our group has achieved fine SK structure successfully in the injection-molded bars of HDPE/inorganic whisker[26,27] and HDPE/MWCNT composites.[28] The composites were prepared through a so-called dynamic packing injection molding (DPIM) technique. The DPIM technique is a special and rare molding method; a detailed description can be found in our previous studies. In order to certify and extend the validity of SK-induced mechanical reinforcement, it is anticipated that a simple and universal processing method is needed to yield SK structure directly in the as-prepared polymer/CNT composites.

Therefore, we report a simple but efficient way to achieve good dispersion and strong interfacial interaction through the melt spinning technique. HDPE/MWCNT composites are used as an example. An almost 3 times increase in tensile strength has been achieved in the fiber containing CNTs fabricated upon high draw ratio compared with the pure HDPE fiber. The formation of well-defined SK structure fabricated upon high draw ratio, with MWCNTs serving as the shish and PE lamellae as the kebab, is considered to be responsible for the enhanced interfacial interaction and improved tensile strength. Particularly, a unique SK network is detected in the as-spun fiber for composites containing 5 wt % MWCNTs. It is believed that the formation of such a structure could enhance the interfacial adhesion and facilitate stress transfer between PE and CNTs significantly. This study is important and may encourage the attempt to prepare polymer composites with novel SK structure for superior mechanical reinforcement.

2. Experimental Section

2.1. Materials and Sample Preparation. The commercially available HDPE trademarked as 2911 with $M_w = 1.3 \times 10^5$ g/mol and polydispersity 3.2 was supplied by Fushun Petrochemical Corp., and used as a matrix resin. The raw MWCNTs were purchased form Shenzhen Nanotechnology Co. Ltd. Its diameter varies from 10 to 20 nm, and its length is in the range 5−15 μm; the purity is approximate 98% and contains less than 0.2% catalyst residue. MWCNTs were used as received without any chemical modification.

Raw MWCNTs were dried at 70 °C in a vacuum for 12 h before compounding. The melt compounding of HDPE and MWCNTs was conducted on a corotating twin-screw extruder (TSSJ-25) with a barrel temperature of 160 °C and a screw speed of 110 rpm; the mass percentages of MWCNTs in the prepared composites are 0.5, 1, 3, and 5 wt %, respectively.

The composites were melt spun as monofilaments at 145 °C using a set of melt spinning device adapted to the piston-mode Rosand RH70 (Malvern, Bohlin Instruments) capillary rheometer. The capillary has a die diameter of 1.0 mm and length-to-diameter ratio of 16. The extruded fibers were air-cooled and picked up under tension by a windup spool. To prepare fibers with different draw ratios (defined as the section area of capillary die versus that of fiber), three take-up speeds were selected. The draw ratio is about 150 for high take-up speed and 50 and 4 for medium and low take-up speed, respectively. In a succinct manner, the as-spun fibers were labeled as *x*CPE-L/M/H, where *x* represents the mass percentage of MWCNTs and L/M/H represents low/medium/high draw ratio, respectively. For instance, 3CPE-H denotes the fiber containing 3 wt % MWCNTs prepared upon high draw ratio. For comparison purposes, the fibers of pure HDPE have also been prepared using the same conditions described above. And these neat PE fibers are marked as PE-L/M/H.

2.2. Characterizations and Measurement. The tensile experiments were carried out on an Instron 5567 universal testing machine with a 100 N-load cell. The fibers were fixed on a paper frame and tested with a crosshead speed of 50 mm/min. The gauge length was 10 mm, and the measured temperature was around room temperature (23 °C). The reported values were calculated as averages over five specimens for each composite.

Microscopic morphology observations were conducted on an FEI Inspect F scanning electron microscope (SEM) under an acceleration voltage of 20 kV. Two types of SEM measurement were adopted for identifying crystalline structure and MWCNT dispersion, respectively. For crystalline structure observation, the fibers were first etched by boiled cyclohexane to remove the amorphous phase of HDPE and then the cylindrical surfaces of the fibers were coated with gold. In another method, the fibers without a gold coating were exposed under electron beam and observed directly with SEM in order to observe MWCNT dispersion in HDPE matrix. The bundles of CNTs can be distinguished from PE matrix due to the prominent difference of electric conductivity between CNTs and PE. A similar method has been used to characterize the morphology of CNTs in polymer matrix elsewhere.[29]

A Perkin-Elmer Pyris I differential scanning calorimeter (DSC) with nitrogen as the purge gas was used to investigate the melting and crystallization behaviors of these fibers. The mass of the specimen was about 5 mg. The sample was first heated to 190 °C at a heating rate of 10 °C/min, holding for 5 min to eliminate any thermal history, and then cooled down to 43 °C at a rate of 10 °C/min. The crystallinity (X_c) of the samples was calculated from the equation $X_c = \Delta H_i/\varphi_i \Delta H_i^m$, where ΔH_i is the enthalpy of fusion, φ_i the weight fraction of polymer, and ΔH_i^m the enthalpy of fusion for 100% crystalline PE, which is adopted as 293 J/g.[30]

Polarized Raman spectroscopy was implemented using a micro-Raman spectrometer (Renishaw) equipped with a Leica microscope. The laser with a wavelength of 514.5 nm was excited by a 136 M He^+ resource. The excited laser with a power of 1.1 mW and a spot diameter of 2 μm was used. In order to determine the orientation level of MWCNTs, the dichroism Raman spectra were achieved by recording Raman spectroscopy along two directions normal between each other, which were parallel and perpendicular to the long-axis (length) direction of fiber, respectively. All received spectra have been calibrated by baseline subtraction.

Two-dimensional wide-angle X-ray scattering (2D-WAXS) experiments were conducted on a Rigaku Denki RAD-B diffractometer. The wavelength of the monochromated X-ray from Cu Kα radiation was 0.154 nm, and the sample-to-detector distance was 273 mm. The samples were placed with the orientation (drawing direction) perpendicular to the beams. The background of all the 2D WAXS patterns given in this Article had been extracted and thus allows a qualitative comparison between various samples. Azimuthal scans (0−360°) 2D WAXS

Figure 1. Photograph of the melt-spun fibers of the HDPE/MWCNT composite containing 5 wt % CNT (the draw ratio varies as the sequence of low-to-medium-to-high from left side to right side).

were made for the (110) plane of PE at a step of 1°. The orientation degree of crystal planes could be calculated by the orientation parameter f from the following equation:

$$f = \frac{3\langle\overline{\cos^2\varphi}\rangle - 1}{2} \quad (1)$$

$$\langle\overline{\cos^2\varphi}\rangle = \frac{\int_0^{\pi/2} I(\phi)\sin\phi\cos^2\phi\,d\phi}{\int_0^{\pi/2} I(\phi)\sin\phi\,d\phi} \quad (2)$$

where φ is the angel between the normal of a given (h k l) crystal plane and the drawing direction and I is the intensity.

3. Results and Discussion

3.1. Tensile Measurements. A photograph exhibiting the typical appearance of the melt-spun fibers is presented in Figure 1. The diameter of the fiber decreases dramatically with increasing draw ratio. No defeat or protuberance can be detected on the fiber surface. Some typical stress−strain curves of neat HDPE and HDPE/MWCNT composites prepared upon different draw ratios are shown in Figure 2. The characteristic tensile behaviors of these fibers at different draw ratios will be discussed as the following. In general, the tensile strength is proportional to the MWCNT content for all draw ratios. For low draw ratio, the mechanical reinforcement of MWCNTs is very limited. The tensile strength is improved from 19.7 to 26.1 MPa, and the improvement in tensile strength is only 32% when the CNT content varies from 0 to 5 wt %. However, the strain at break decreases dramatically with increasing MWCNT content, and a strain at break of 20% is obtained for 5CPE-L. The mechanical properties are similar to those of isotropic

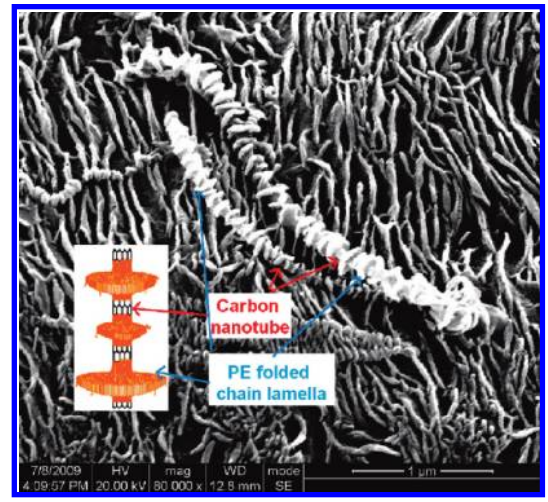

Figure 3. Typical shish-kebab superstructure that is existent in the melt-spun HDPE/MWCNT fibers. (The drawings are not to scale.)

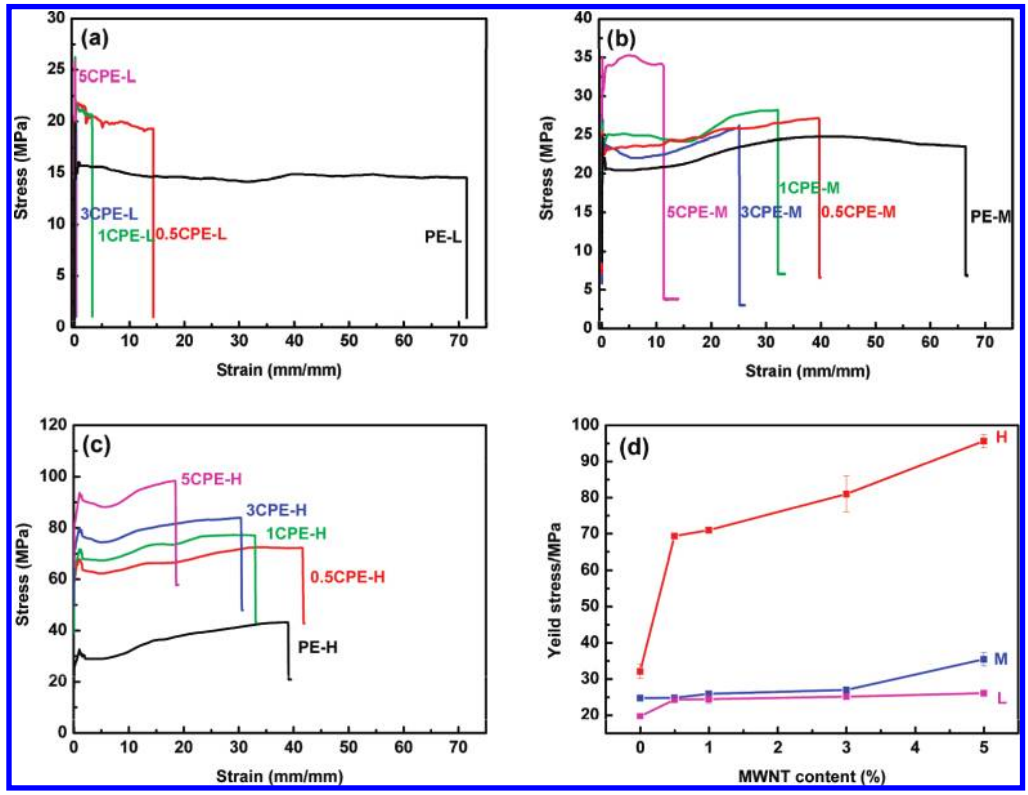

Figure 2. Stress−strain curves of the HDPE/MWCNT fibers at different MWCNT loadings prepared upon different draw ratios: (a) low draw ratio; (b) medium draw ratio; (c) high draw ratio. (d) Tensile properties of the composite fibers with different CNT contents.

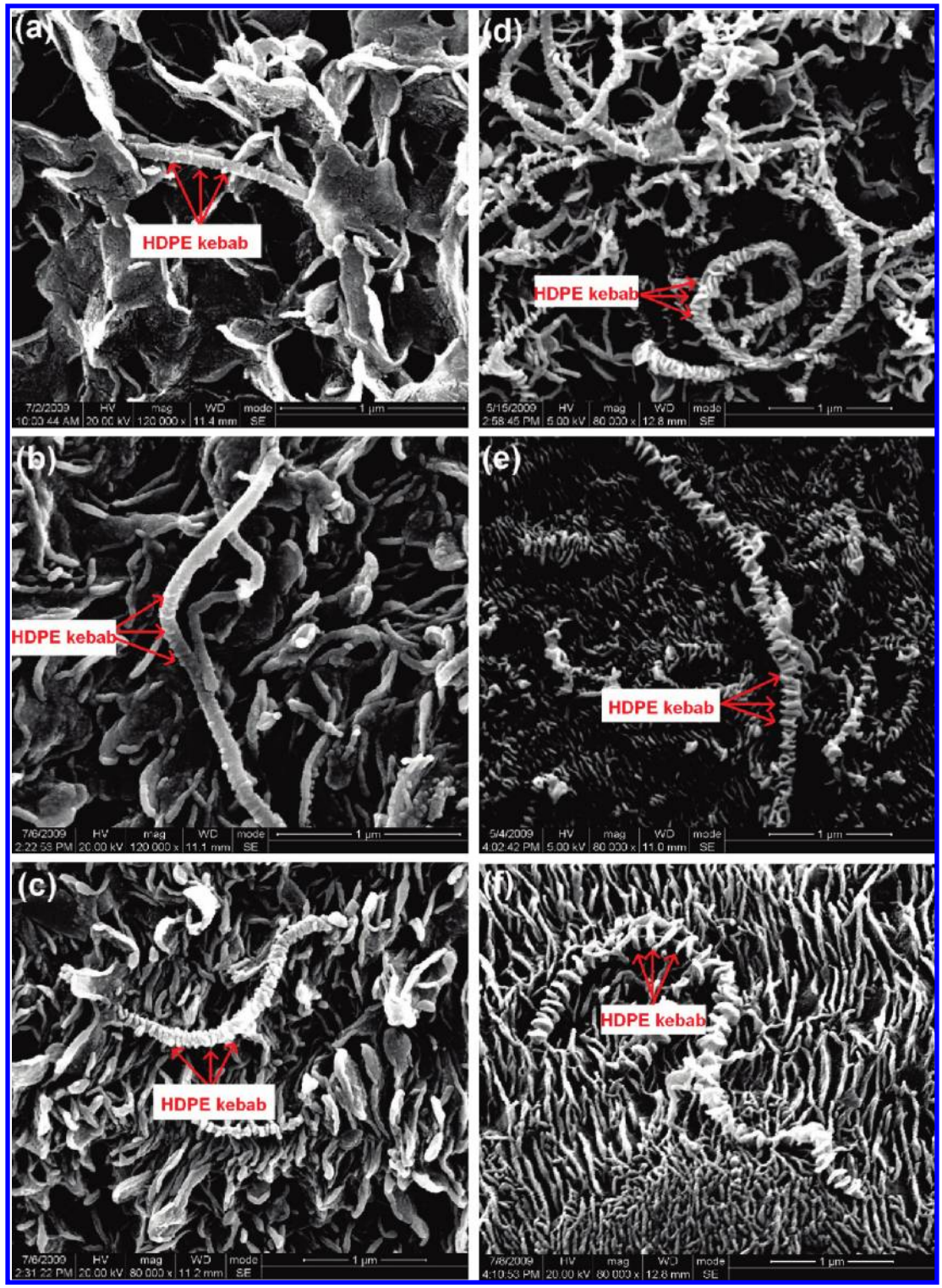

Figure 4. SEM micrographs of shish-kebab structure in the composites taken parallel to the flow direction: (a) 0.5CPE-L; (b) 0.5CPE-M; (c) 0.5CPE-H; (d) 5CPE-L; (e) 5CPE-M; (f) 5CPE-H.

HDPE/CNT composites. For medium draw ratio, the tensile strength is improved from 24.8 to 35.5 MPa with increasing CNT content from 0 to 5 wt %; therefore, an increase of 43% is obtained. It is interesting to note that in this case the strain at break can be partially preserved for 5CPE-M, as it only decreases from 6660 to 1400% when 5 wt % MWCNTs were added into the system.

Superior mechanical reinforcement is achieved in a series of fibers fabricated at high draw ratio. The efficiency of mechanical enhancement is prominently better than those fibers obtained at low or medium draw ratios. An extraordinary increase in tensile strength of 198% is obtained for fibers containing 5 wt % CNTs. Meanwhile, the strain at break of 5CPE-H is maintained at 1970%, which is comparable to that of PE-H (4140%). Obviously, increase of draw ratio is beneficial for both strength and toughness of these fibers. The values of tensile strength are extracted from the stress−strain curves and plotted as a function of CNT content in Figure 2d. One can clarify the trends of tensile strength with variations in draw ratio and CNT content. The mechanisms of superior mechanical reinforcement

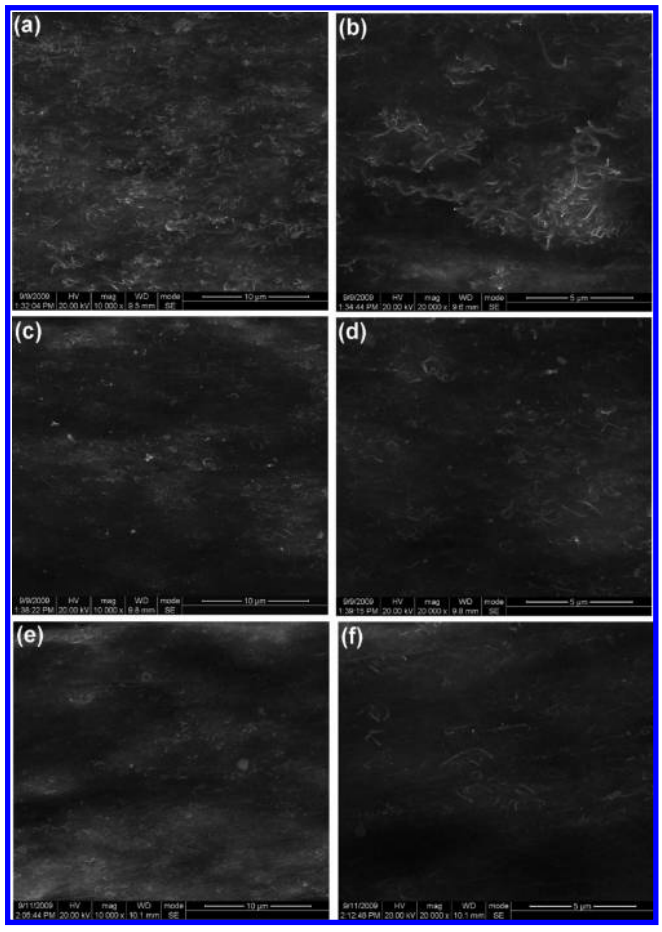

Figure 5. SEM images representing the dispersion of CNTs in the composite fiber at low magnification (×10 000) (left) and high magnification (×20 000) (right): (a, b) 5CPE-L; (c, d) 5CPE-M; (e, f) 5CPE-H.

will be discussed in detail associating with the following morphological and structural investigations.

3.2. Shish-Kebab Structure in Melt-Spun Fibers. The crystalline structure in melt-spun fibers can be clearly distinguished after chemical etching as the amorphous phase of HDPE is removed during etching. A micrograph of crystalline structure in the 5CPE-H fiber is shown in Figure 3, where two entities of well-defined SK are observed as indicated by the arrows. The structural features of shish-kebab are as follows: the filament of CNT acted as the shish, while the PE single crystal lamellae serve as kebabs, and a CNT shish is decorated with many PE kebabs in the lateral direction of PE lamellae (approximately perpendicular to the long axis of CNT). In Figure 3, the stretching direction of fiber is horizontal. However, the SK structures are not aligning along the stretching direction; instead, the CNT shish obviously inclines away from the horizontal direction. This phenomenon was also found in the injection-molded bar of HDPE/MWCNT composites.[28] No matter if the long axis of CNT is parallel or biased to the stretching direction, the lamellae of PE are always perpendicular to the long axis of CNT, indicating a strong epitaxial growth of PE on the sidewalls of CNTs. The formation of SK structure observed in the HDPE/CNT composites in our previous work is most likely induced by the shear force caused by injection molding. Here, we present another example that the SK structure could also be induced by stretching force during melt spinning.

Similar to the tensile properties, the structure of SK in the melt-spun fibers is impacted substantially by the content of MWCNTs and draw ratio (see Figure 4). For MWCNT content of 0.5 wt %, there are only some globules or protuberances that attach loosely on the sidewalls of MWCNTs in the fiber obtained at low draw ratio, such as 0.5CPE-L. These globules or protuberances can be regard as incomplete or prime kebabs. With increasing draw ratio, the prime kebabs become more obvious but still incomplete and the profile of MWCNT can be

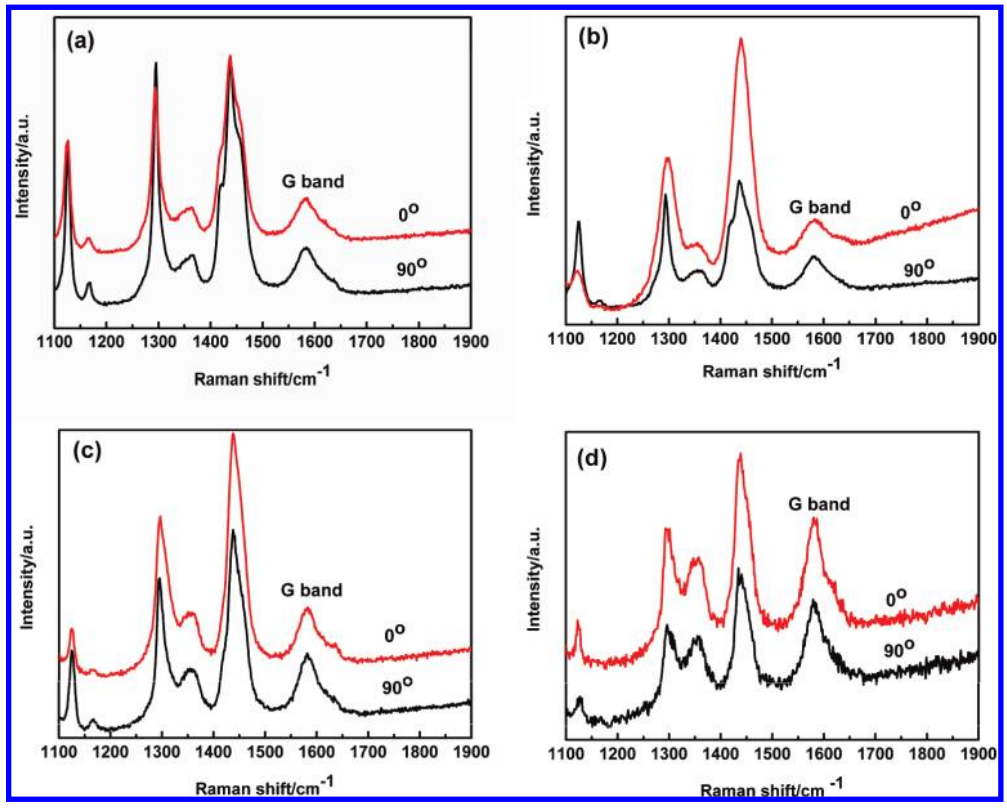

Figure 6. Polarized Raman spectra of composite fiber: (a) 0.5CPE-L; (b) 0.5CPE-H; (c) 5CPE-L; (d) 5CPE-H.

TABLE 1: The *R* Values of Fiber Derived from the Dichroism Raman Spectra

	0.5CPE-L	0.5CPE-H	5CPE-L	5CPE-H
R	0.96	1.09	0.95	1.30

seen clearly in the fiber from 0.5CPE-M, while the PE kebabs are distinct and grow densely on the sidewall of MWCNT in the fiber from 0.5CPE-H. The structure obtained there can be regarded as a fine SK structure. For high MWCNT content (5 wt %), the well-defined SK structures are obtained for all draw ratios. However, the complete level of SK is somewhat different between these draw ratios.

In the fiber of 5CPE-L, the PE kebabs are thin and short, and many kebabs cannot wrap around the filament of MWCNT completely. This indicates that such kebabs are only preliminary kebabs. In the fiber of 5CPE-M, all PE kebabs can cincture the whole section area of MWCNTs, which indicates that the PE kebabs become more complete than that at low draw ratio. Particularly, the thickness and lateral length of PE kebabs in the fiber of 5CPE-H are prominently larger than those in the 5CPE-M fiber. Thus, the finest SK structure is achieved in the fiber containing 5 wt % MWCNT and fabricated at high draw ratio. Therefore, increasing MWCNT content and draw ratio plays positive roles on the formation of fine SK structure. A similar trend is observed for the relationship between tensile strength and these two factors.

3.3. Dispersion of MWCNTs in Composites. It has been widely reported that shearing, particularly upon high shear rate, can usually result in a better dispersion of filler in polymer matrix.[31] In order to confirm the effect of draw ratio on the dispersion of MWCNTs in the fiber, in situ microscopic observation of MWCNTs is implemented directly on the melt-spun fiber containing 5 wt % MWCNTs. Under electron irradiation, MWCNTs were whitened while the PE matrix darkened, due to the excellent electric conductivity of carbon nanotube at high loading.

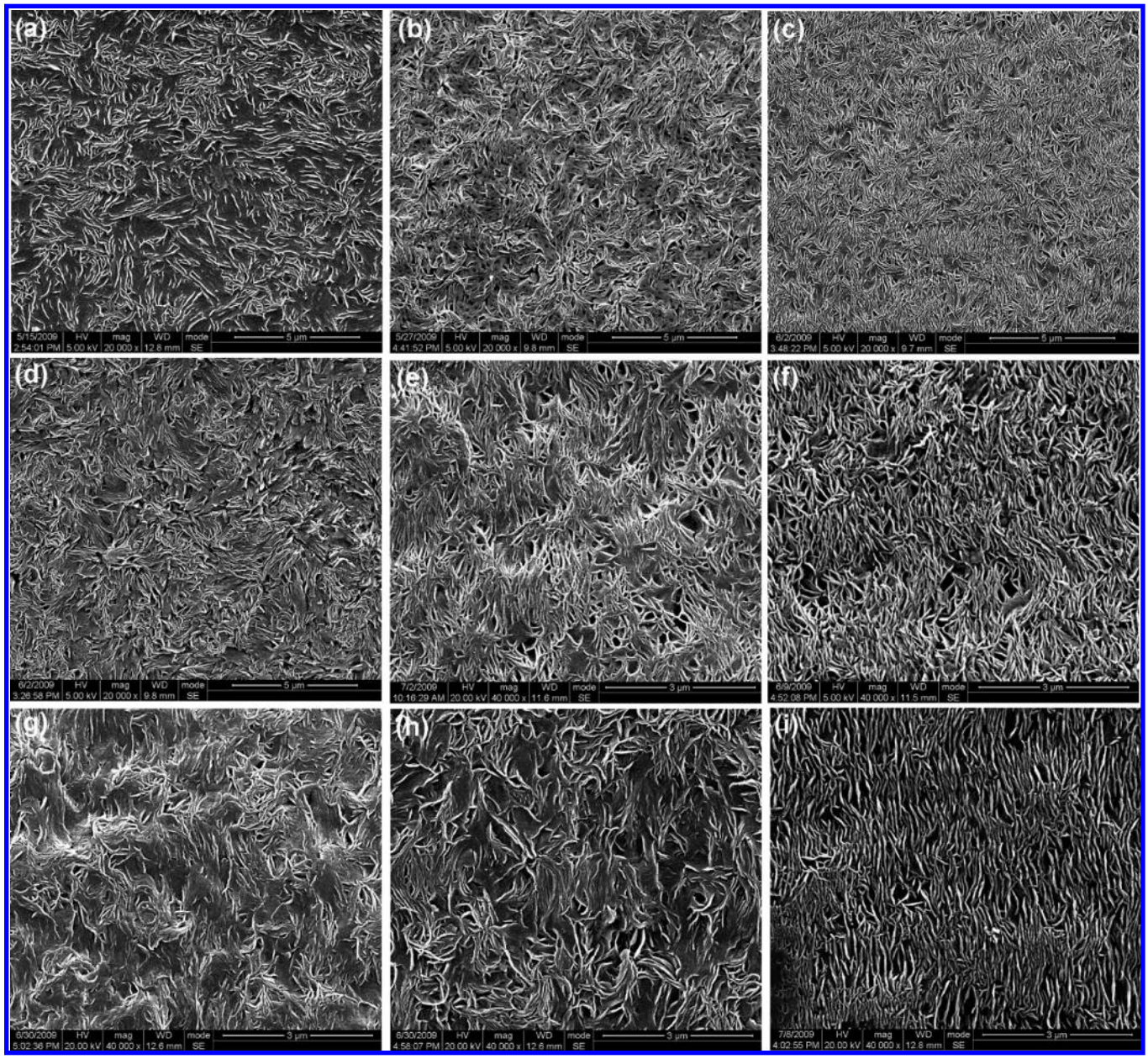

Figure 7. SEM images representing the crystallization morphology along the flow direction: (a) PE-L; (b) 0.5CPE-L; (c) 5CPE-L; (d) PE-M; (e) 0.5CPE-M; (f) 5CPE-M; (g) PE-H; (h) 0.5CPE-H; (i) 5CPE-H.

As shown in Figure 5, the filaments and coils of MWCNTs appear everywhere within the whole observation area for three draw ratios. However, the dispersion levels of MWCNTs are different between three draw ratios through observation under high magnification (×20 000). Aggregations and blocks of MWCNTs can be observed at low draw ratio, coalescence of MWCNTs reduces substantially at medium draw ratio, and the best dispersion of MWCNTs is obtained for high draw ratio as numerous individual filaments of MWCNT are observed. It is believed that the high shear rate caused by high draw ratio can reduce the amount of MWCNT aggregations. Moreover, a tendency of slight orientation can be detected in the fiber obtained by high draw ratio, as CNTs would rather align along the stretching direction.[32−34] The anisotropy of the MWCNT framework in the melt-spun fiber will be estimated quantitatively by Raman spectroscopy.

3.4. Orientation Structure in Melt-Spun Fibers. The polarized Raman spectra of 0.5CPE-L, -H, and 5CPE-L, -H are shown in Figure 6. For each sample, the Raman spectra are recorded parallel to (0°) and perpendicular to (90°) the stretching direction of fiber. As shown in Figure 6, the characteristic peak of the CNT D band located at 1345 cm^{-1} has been superposed by the PE signal completely, whereas the G band peak (tangential mode) at 1580 cm^{-1} can be distinguished clearly from the PE signal, which represents the undisturbed CNT behavior. To evaluate the anisotropy of the MWCNT framework, the depolarization factor (dichroistic factor), R, has been adopted. It is defined as the ratio of the peak intensity for the G band in the parallel direction ($I_0°$) to that in the perpendicular direction ($I_{90}°$), $I_0°/I_{90}°$. The calculated values of R are listed in Table 1. An R value close to unity indicates an isotropic morphology, whereas a value higher than unity implies preferential orientation along the fiber stretching direction. For both contents of 0.5 and 5 wt %, increasing draw ratio can indeed promote anisotropy of MWCNTs.

The MWCNT framework is approximately isotropic when the draw ratio is low, while the value of R is larger than unity for the sample obtained at high draw ratio. Nevertheless, the increase of anisotropy for 0.5 wt % MWCNT is very limited, as it only increases from 0.96 to 1.09. A relatively high anisotropy (1.3) is achieved in the 5CPE-H fiber, which is consistent with the result shown in Figure 5.

The orientation of HDPE matrix has been investigated by SEM. Some representative micrographs are shown in Figure 7. For neat HDPE and composite containing 0.5 wt % MWCNT, only isotropic spherulites can be observed for all of the draw ratios. This indicates that a low orientation level of the matrix crystalline phase is obtained in these fibers. For the composites containing 5 wt % MWCNT, the matrix crystalline morphology is transformed from spherulitic (isotropic) to oriented (anisotropic) with increasing draw ratio. For instance, the lamellae of PE arrange orderly with their lateral direction perpendicular to the stretching direction (the horizon) in the fiber of 5CPE-H. For neat HDPE, a higher draw ratio usually causes a higher orientation. However, a low degree of orientation is observed for neat HDPE due to the low molecular weight HDPE that was used in our work. The orientation obtained may be easily reduced by relaxation. This can also be observed from the limited enhancement in tensile strength of neat HDPE after stretching. For HDPE/MWCNT composites, the increased orientation of HDPE upon drawing is caused by the increased alignment of MWCNTs (this is supported by polarized Raman spectroscopy). The strong tendency of epitaxy growth of PE on the sidewall of MWCNTs results in not only the formation of shish-kebab structure but also a largely increased orientation of HDPE. A further determination of HDPE orientation for the melt-spun fibers was carried out using 2D-WAXS. As shown in Figure 8, the scattering signals are designated to the (110) plane and (200) plane of orthorhombic PE lamellae. The orientation degree of all samples obtained from 2D-WAXS patterns is listed in Table 2. A low orientation level of the matrix crystalline phase is evident in all fibers. It can be noted that the anisotropic degree of scattering arcs is enhanced for the crystalline planes for all of the draw ratios with increasing MWCNT content. For the fibers containing 0, 0.5, and 5 wt % MWCNT, the orientation degree of the (110) plane is 0.33, 0.40, and 0.50 for low draw ratio and 0.41, 0.44, and 0.58 for high draw ratio, respectively. Furthermore, the effect of draw ratio on the structural orientation can be estimated by comparing the top images to the bottom ones. The orientation level increases slightly with increasing draw ratio. The quantitative estimation of orientation suggests that the effect of increasing draw ratio on the oriented degree of crystalline structure is not significant. Nevertheless, the more MWCNT the system contains, the higher orientation that is achieved. It might be caused by the higher viscosity obtained for highly loaded composites; thus, higher shear is experienced by the fiber during melt spinning. Such an improved polymer chain orientation might play a role on the mechanical properties in conjunction with SK structure and MWNT morphology.

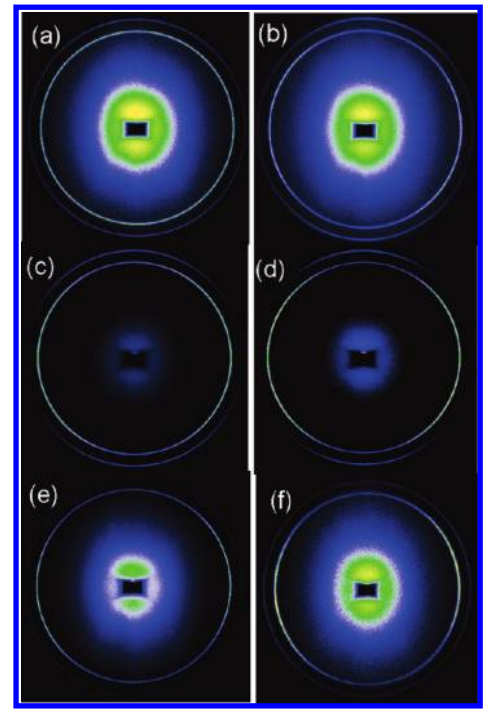

Figure 8. 2D-WAXS patterns of the HDPE/MWCNT composites: (a) PE-L; (b) PE-H; (c) 0.5CPE-L; (d) 0.5CPE-H; (e) 5CPE-L; (f) 5CPE-H.

TABLE 2: Oriented Degrees of Various Draw Ratios of HDPE/MWCNT Composites Obtained by 2D-WAXS

	orientation degree		
	HDPE	0.5 wt % MWCNT	5 wt % MWCNT
low draw ratio	0.33	0.40	0.50
high draw ratio	0.41	0.44	0.58

3.5. Calorimetric Analysis. The melting and subsequent crystallization curves of the melt-spun fibers are presented in Figure 9. The values including melt temperature (T_m), crystal-

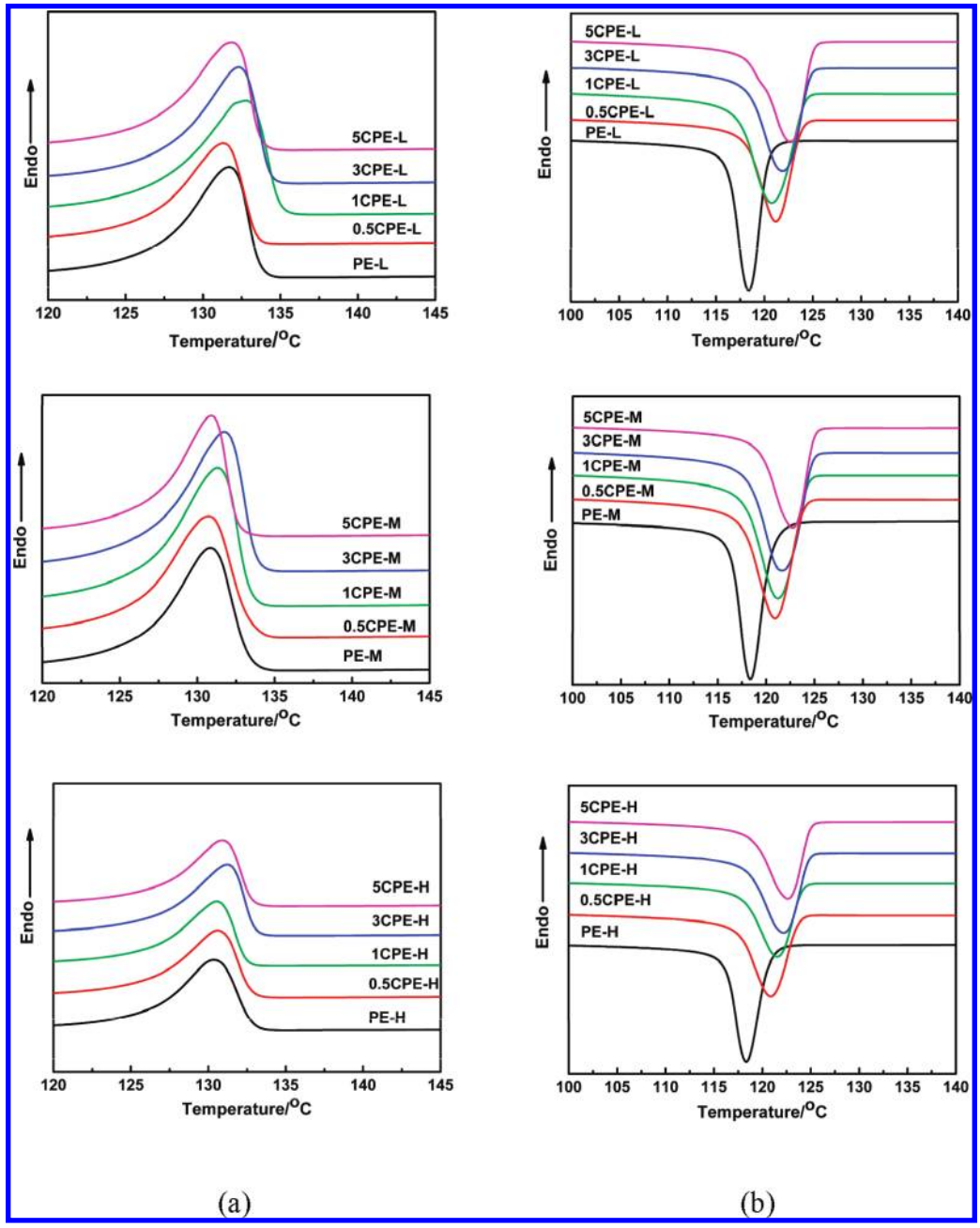

Figure 9. DSC melting curves (a) and subsequently nonisothermal crystallization curves (b) of the melt-spun fibers of the pure HDPE and the HDPE/MWCNT composites.

TABLE 3: Nonisothermal Crystallization and Melting Data of the Samples (T_c, Crystallization Peak Temperature; T_m, Melting Peak Temperature; X_c, wt % Crystallinity of HDPE)

	L			M			H		
wt %	T_c (°C)	T_m (°C)	X_c (%)	T_c (°C)	T_m (°C)	X_c (%)	T_c (°C)	T_m (°C)	X_c (%)
0	118.4	131.6	64.2	118.3	130.8	58.8	118.4	130.3	58.6
0.5	121.2	131.4	60.6	120.9	130.7	59.1	120.8	130.6	58.8
1	120.8	132.8	63.9	121.2	131.4	62.7	121.6	130.6	60.5
3	121.9	132.4	63.9	121.7	131.7	62.1	122.2	131.2	61.2
5	122.8	131.8	61.2	122.7	130.9	59.1	122.7	130.9	60.2

linity (X_c), and crystallization temperature (T_c), are listed in Table 3. One can observe a relatively constant T_m with increasing MWCNT content is obtained for all draw ratios. A similar behavior is detected for the crystallinity. On the other hand, the cooling crystallization behaviors are similar for all draw ratios: T_c is increased from near 118.4 °C for pure PE to near 122.7 °C for 5 wt % MWCNT. The increase in T_c with additional CNTs indicates a heterogeneous nucleation effect to facilitate HDPE crystallization. Therefore, it is believed that the crystallization begins from the sidewalls of MWCNTs.

3.6. Effect of SK Structure on Reinforcement of Melt-Spun Fiber. It can be envisaged that the macroscopic mechanical performance of melt-spun fibers is influenced by many structural and morphological factors, such as SK structure (PE/

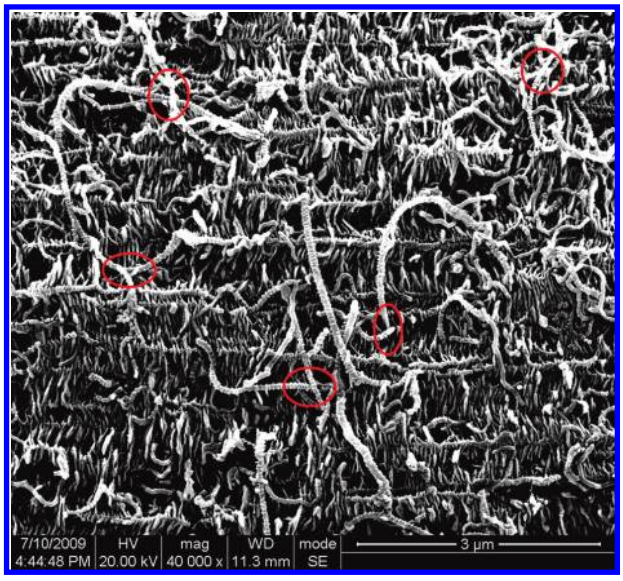

Figure 10. Micrographs demonstrating the SK network embedded in PE matrix in the melt-spun fiber containing 5 wt % MWCNT fabricated upon high draw ratio.

MWCNT interaction), dispersion of MWCNTs, orientation of MWCNTs and matrix crystalline phase, and crystalline properties (lamellar thickness, crystallinity). According to the DSC results, the effect of CNT content on lamellar thickness (T_m) and crystallinity can almost be ignored. Thus, it can be deduced that the crystalline properties do not contribute to mechanical reinforcement in the as-prepared fibers. It has been revealed that the fiber of 5CPE-H possesses good MWCNT dispersion, anisotropic MWCNT framework, and high level of PE matrix orientation. They are all favorable for mechanical reinforcement. To further investigate the superior mechanical reinforcement obtained in detail, we would like to focus on a series of fibers containing 0.5 wt % MWCNT, in which the CNT dispersion and orientation structure are almost unchanged with different draw ratios. However, the tensile strength is improved by 186%: increase from 24.3 MPa (for low draw ratio) to 69.4 MPa (high draw ratio). The structural and morphological factor that alters substantially with an increase of draw ratio is the SK structure. As shown in Figure 4, the SK structure becomes more complete with increasing draw ratio. Thus, the mechanical enhancement in the fiber containing 0.5 wt % MWCNT can be mainly attributed to the formation of fine SK structures while fabricating melt-spun fiber under shear. In the fiber of 5CPE-H, the PE kebabs are thicker and longer, and the perfectibility of the SK entity is better than that in the fiber of 0.5CPE-H. It is expected that the enhancement effect of SK is stronger in the fiber of 5CPE-H. This expectation is supported by a dramatic increase in tensile strength by 267% (from 26.1 MPa for 5CPE-L to 95.7 MPa for 5CPE-H). Other factors also contribute to this increase in strength, but SK structure plays a more dominant and essential role on the mechanical reinforcement in the melt-spun fibers.

It is believed that the mechanism of SK entities strengthens the property of PE matrix is attributed to enhancement of interfacial adhesion and stress transfer between PE and CNTs. This explanation only takes an individual SK entity into account, where the influence of the networks and interactions between numerous SK entities is ignored. The 5 wt % content of MWCNTs is higher than the percolation threshold needed for forming a MWCNT network in PE matrix (which is 3 wt % as determined by melt rheometry[28]). As shown in Figure 10, the SK entities are abundant for the fiber of 5CPE-H. Importantly, a unique SK network has been constructed in this fiber, since many SK entities crosshatched and entangled together. The cross-linking sites of SK entities are highlighted by circles on the micrographs of Figure 10. Obviously, the formation of the SK network makes the reinforcement of SK more effective in the fiber of 5CPE-H.

In order to improve the interfacial adhesion between CNTs and polymer matrix, many complicated methods have been developed to modify and disperse CNTs. Nevertheless, the reinforcing efficiency is not as good as expected in most cases. In our work, a great improvement of tensile strength is achieved merely through a simple processing method of melt spinning. The key is to promote the formation of novel SK structure. This is important and valuable to expand the application of SK structure in the CNT composites fabricated by melt processing strategy.

It is also interesting to notice that the increase in tensile strength is accompanied by improvement of ductility (toughness) in the as-prepared fibers. For example, the strain at break is increased from 20% (for low draw ratio) to 1970% (for high draw ratio) for the fibers containing 5 wt % MWCNTs. This is an unusual mechanical behavior that differs from common composites, where the ductility decreases rapidly with strengthening. Simultaneously strengthening and toughening nanofiller filled composites have been reported in highly oriented injection-molded bars of PE/MWCNT composites.[35] The improvement of toughness in highly oriented composites with nanoparticles can be attributed to the motion of nanoparticles under stretching deformation, which can induce more energy dissipation.[36,37] In the melt-spun fibers, MWCNTs and HDPE matrix are bonded together by SK structure. It is favorable for the stress transfer and easy motion of MWCNTs during tensile deformation. Therefore, the formation of SK structure can cause excellent mechanical properties, and simultaneous toughening and strengthening is observed in the melt-spun fibers.

4. Conclusions

Melt spinning is an efficient way to produce SK structure for HDPE/MWCNT composites. An extraordinary mechanical reinforcement has been achieved in the melt-spun HDPE/MWCNT fibers. This reinforcement effect is mainly attributed to the formation of fine SK structure during the melt spinning process. Nevertheless, the orientation of the polymer chain may also influence the mechanical properties of the composites in conjunction with the effect of SK structure and orientation of MWNTs. According to the microscopic observations, increasing MWCNT content and draw ratio are favorable for obtaining perfect SK structure. Moreover, a unique SK network is detected in the as-spun fiber for composites containing 5 wt % MWCNTs. It is believed that the formation of such a structure could enhance the interfacial adhesion and facilitate stress transfer between PE and CNTs significantly. This study is important and may encourage the attempt to prepare polymer composites with novel SK structure for superior mechanical reinforcement. Furthermore, the effect of matrix molecular weight and its distribution on the effect described above is currently under investigation, since the chain mobility plays a very important role on the dispersion and the formation of SK in polymer/CNT composites.

Acknowledgment. We express our sincere thanks to the National Natural Science Foundation of China for financial support (50533050, 20874064, 50873063). The authors gratefully acknowledge the help of Ms. Xinyuan Zhang of the Analytical and Testing Center at Sichuan University for the SEM micrographs.

References and Notes

(1) McIntosh, D.; Khabashesku, V. N.; Barrera, E. V. Benzoyl Peroxide Initiated In Situ Functionalization, Processing, and Mechanical Properties of Single-Walled Carbon Nanotube-Polypropylene Composite Fibers. *J. Phys. Chem. C* **2007**, *111*, 1592–1600.

(2) Geng, H.; Rosen, R.; Zheng, B.; Shimoda, H.; Fleming, L.; Liu, J.; Zhou, O. Fabrication and Properties of Composites of Poly(ethylene oxide) and Functionalized Carbon Nanotubes. *Adv. Mater.* **2002**, *14*, 1387–1390.

(3) Gao, J.; Itkis, M. E.; Yu, A.; Bekyarova, E.; Zhao, B.; Haddon, R. C. Continuous Spinning of a Single-Walled Carbon Nanotube-Nylon Composite Fiber. *J. Am. Chem. Soc.* **2005**, *127*, 3847–3854.

(4) Choi, E. S.; Brooks, J. S.; Eation, D. L.; Al-Haik, M. S.; Hussaini, M. Y.; Garmestani, H.; Li, D.; Dahmen, K. Enhancement of thermal and electrical properties of carbon nanotube polymer composites by magnetic field processing. *J. Appl. Phys.* **2003**, *94*, 6034–6039.

(5) Xu, J. W.; Florkowski, W.; Gerhardt, R.; Moon, K.; Wong, C. P. Shear Modulated Percolation in Carbon Nanotube Composites. *J. Phys. Chem. B* **2006**, *110*, 12289–12292.

(6) Zhang, D.; Kandadai, M. A.; Cech, J.; Roth, S.; Curran, S. A. Poly(L-lactide) (PLLA)/Multiwalled Carbon Nanotube (MWCNT) Composite: Characterization and Biocompatibility Evaluation. *J. Phys. Chem. B* **2006**, *110*, 12910–12915.

(7) Park, S.; Yoon, S. W.; Choi, H.; Lee, J. S.; Cho, W. K.; Kim, J.; Park, H. J.; Yun, W. S.; Choi, C. H.; Do, Y.; Choi, I. S. Pristine Multiwalled Carbon Nanotube/Polyethylene Nanocomposites by Immobilized Catalysts. *Chem. Mater.* **2008**, *20*, 4588–4594.

(8) Yang, B. X.; Pramoda, K. P.; Xu, G. Q.; Goh, S. H. Mechanical Reinforcement of Polyethylene Using Polyethylene-Grafted Multiwalled Carbon Nanotubes. *Adv. Funct. Mater.* **2007**, *17*, 2062–2069.

(9) Blake, R.; Gun'ko, Y. K.; Coleman, J.; Cadek, M.; Fonseca, A.; Nagy, J. B.; Blau, W. J. A Generic Organometallic Approach toward Ultra-Strong Carbon Nanotube Polymer Composites. *J. Am. Chem. Soc.* **2004**, *126*, 10226–10227.

(10) Lu, K. B.; Grossiord, N.; Koning, C. E.; Miltner, H. E.; Mele, B. V.; Loos, J. Carbon Nanotube/Isotactic Polypropylene Composites Prepared by Latex Technology: Morphology Analysis of CNT-Induced Nucleation. *Macromolecules* **2008**, *41*, 8081–8085.

(11) Chen, Q. Y.; Bin, Y. Z.; Matsuo, M. Characteristics of Ethylene-Methyl Methacrylate Copolymer and Ultrahigh Molecular Weight Polyethylene Composite Filled with Multiwall Carbon Nanotubes Prepared by Gelation/Crystallization from Solutions. *Macromolecules* **2006**, *39*, 6528–6536.

(12) Zhang, Q. H.; Rastogi, S.; Chen, D.; Lippits, D.; Lemstra, P. J. Low percolation threshold in single-walled carbon nanotube/high density polyethylene composites prepared by melt processing technique. *Carbon* **2006**, *44*, 778–785.

(13) Xiao, K. Q.; Zhang, L. C.; Zarudi, I. Mechanical and rheological properties of carbon nanotube-reinforced polyethylene composites. *Compos. Sci. Technol.* **2007**, *67*, 177–182.

(14) Ganβ, M.; Satapathy, B. K.; Thunga, M.; Weidisch, R.; Potschke, P.; Jehnichen, D. Structural interpretations of deformation and fracture behavior of polypropylene/multi-walled carbon nanotube composites. *Acta Mater.* **2008**, *56*, 2247–2261.

(15) McNally, T.; Potschke, P.; Halley, P.; Murphy, M.; Martin, D.; Bell, S. E. J.; Brennan, G. P.; Bein, D.; Lemoine, P.; Quinn, J. P. Polyethylene multiwalled carbon nanotube composites. *Polymer* **2005**, *46*, 8222–8232.

(16) Bhattacharyya, A. R.; Sreekumar, T. V.; Liu, T.; Kumar, S.; Ericson, L. M.; Hauge, R. H.; Smalley, R. E. Crystallization and orientation studies in polypropylene/single wall carbon nanotube composite. *Polymer* **2003**, *44*, 2373–2377.

(17) Grady, B. P.; Pompeo, F.; Shambaugh, R. L.; Resasco, D. E. Nucleation of Polypropylene Crystallization by Single-Walled Carbon Nanotubes. *J. Phys. Chem. B* **2002**, *106*, 5852–5858.

(18) Probst, O.; Moore, E. M.; Resasco, D. E.; Grady, B. P. Nucleation of polyvinyl alcohol crystallization by single-walled carbon nanotubes. *Polymer* **2004**, *45*, 4437–4443.

(19) Uehara, H.; Kato, K.; Kakiage, M.; Yamanobe, T.; Komoto, T. Single-Walled Carbon Nanotube Nucleated Solution-Crystallization of Polyethylene. *J. Phys. Chem. C* **2007**, *111*, 18950–18957.

(20) Li, C. Y.; Li, L. Y.; Cai, W. W.; Kodjie, S. L.; Tenneti, K. K. Nanohybrid Shish-Kebabs: Periodically Functionalized Carbon Nanotubes. *Adv. Mater.* **2005**, *17*, 1198–1202.

(21) Li, L. Y.; Li, C. Y.; Ni, C. Y.; Rong, L. X.; Hsiao, B. S. Structure and crystallization behavior of Nylon 66/multi-walled carbon nanotube nanocomposites at low carbon nanotube contents. *Polymer* **2007**, *48*, 3452–3460.

(22) Zhang, L.; Tao, T.; Li, C. Z. Formation of polymer/carbon nanotubes nano-hybrid shish-kebab via non-isothermal crystallization. *Polymer* **2009**, *50*, 3835–3840.

(23) Zhang, Z. W.; Xu, Q.; Chen, Z. M.; Yue, J. Nanohybrid Shish-Kebabs: Supercritical CO_2-Induced PE Epitaxy on Carbon Nanotubes. *Macromolecules* **2008**, *41*, 2868–2873.

(24) Li, L. Y.; Li, B.; Hood, M. A.; Li, C. Y. Carbon nanotube induced polymer crystallization: The formation of nanohybrid shish-kebabs. *Polymer* **2009**, *50*, 953–965.

(25) Liang, S.; Wang, K.; Chen, D. Q.; Zhang, Q.; Du, R. N.; Fu, Q. Shear enhanced interfacial interaction between carbon nanotubes and polyethylene and formation of nanohybrid shish−kebabs. *Polymer* **2008**, *49*, 4925–4929.

(26) Ning, N. Y.; Luo, F.; Pan, B. F.; Zhang, Q.; Fu, Q. Observation of Shear-Induced Hybrid Shish Kebab in the Injection Molded Bars of Linear Polyethylene Containing Inorganic Whiskers. *Macromolecules* **2007**, *40*, 8533–8536.

(27) Ning, N. Y.; Luo, F.; Wang, K.; Zhang, Q.; Chen, F.; Du, R. N.; An, C. Y.; Pan, B. F.; Fu, Q. Molecular Weight Dependence of Hybrid Shish Kebab Structure in Injection Molded Bar of Polyethylene/Inorganic Whisker Composites. *J. Phys. Chem. B* **2008**, *112*, 14140–14148.

(28) Yang, J. H.; Wang, C. Y.; Wang, K.; Zhang, Q.; Chen, F.; Du, R. N.; Fu, Q. Direct Formation of Nanohybrid Shish-Kebab in the Injection Molded Bar of Polyethylene/Multiwalled Carbon Nanotubes Composite. *Macromolecules* **2009**, *42*, 7016–7023.

(29) Kovacs, J. Z.; Andresen, K.; Pauls, J. R.; Garcia, C. P.; Schossig, M.; Schulte, K.; Bauhoferet, M. Analyzing the quality of carbon nanotube dispersions in polymers using scanning electron microscopy. *Carbon* **2007**, *45*, 1279–1288.

(30) Na, B.; Wang, K.; Zhang, Q.; Du, R. N.; Fu, Q. Tensile properties in the oriented blends of high-density polyethylene and isotactic polypropylene obtained by dynamic packing injection molding. *Polymer* **2005**, *46*, 3190–3198.

(31) Chen, G. X.; Li, Y. J.; Shimizu, H. Ultrahigh-shear processing for the preparation of polymer/carbon nanotube composites. *Carbon* **2007**, *45*, 2334–2340.

(32) Deng, H.; Zhang, R.; Bilotti, E.; Loos, J.; Peijs, T. Conductive polymer tape containing highly oriented carbon nanofillers. *J. Appl. Polym. Sci.* **2009**, *113*, 742–751.

(33) Deng, H.; Zhang, R.; Bilotti, E.; Loos, J.; Peijs, T. Effect of thermal annealing on the electrical conductivity of high-strength bicomponent polymer tapes containing carbon nanofillers. *Synth. Met.* **2010**, *160*, 337–344.

(34) Deng, H.; Zhang, R.; Reynolds, C. T.; Bilotti, E.; Peijs, T. A novel concept for highly oriented carbon nanotube composite tapes or fibres with high strength and electrical conductivity. *Macromol. Mater. Eng.* **2009**, *294*, 749–755.

(35) Zhao, P.; Wang, K.; Yang, H.; Zhang, Q.; Du, R. N.; Fu, Q. Excellent tensile ductility in highly oriented injection-molded bars of polypropylene/carbon nanotubes composites. *Polymer* **2007**, *48*, 5688–5695.

(36) Gersappe, D. Molecular Mechanisms of Failure in Polymer Nanocomposites. *Phys. Rev. Lett.* **2002**, *89*, 058301−1–4.

(37) Shah, D.; Maiti, P.; Jiang, D. D.; Batt, C. A.; Giannelis, E. P. Effect of Nanoparticle Mobility on Toughness of Polymer Nanocomposites. *Adv. Mater.* **2005**, *17*, 525–528.

JP1019944